Jurnal Rekayasa Mesin
p-ISSN: 1411-6863, e-ISSN: 2540-7678
Vol. 19, No. 2, Agustus **2024**, hal. 199-210

Numerical Modelling of NACA 0015 Airfoil Under Erosion Condition

Rayhan Fariansyah Billad[1*], James Julian[1], Fitri Wahyuni[1], Waridho Iskandar[2]
[1]Department of Mechanical Engineering , Universitas Pembangunan Nasional Veteran Jakarta,
Jl. Rs. Fatmawati, Pondok Labu, Jakarta Selatan, DKI Jakarta, 12450
[2] Fluid Mechanics Labroratory, University Indonesia,
Kampus Baru UI, Depok 16424, Jawa Barat, Indonesia

*E-mail: zames@upnvj.ac.id

Diajukan: 27-09-2023; Direvisi: 20-08-2024; Dipublikasi: 31-08-2024

Abstrak

Airfoil yang mengalami erosi dengan variasi bilangan *Reynolds* diteliti menggunakan metode numerik untuk mengetahui efek tersebut terhadap performa *airfoil* NACA 0015. Penelitian ini disimulasikan menggunakan pendekatan *Computational Fluid Dynamics* (CFD). *Reynolds Averaged Navier-Stokes* (RANS) diimplementasikan sebagai persamaan pengatur tersebut. Model turbulensi yang digunakan pada penelitian ini adalah model k-epsilon. Bilangan *Reynolds* yang digunakan yaitu 1.6 x 10^6, 2 x 10^6, dan 2.5 x 10^6. Penelitian ini membuktikan bahwa efek erosi dapat menurunkan nilai C_l dan meningkatkan nilai C_d pada airfoil NACA 0015. Peningkatan bilangan *Reynolds* juga dapat menurunkan nilai rata-rata C_l dan meningkatkan nilai rata-rata C_d. Penurunan nilai rata-rata C_l masing-masing yaitu 6.561%, 9.392%, dan 9.803% pada bilangan *Reynolds* 1.6 x 10^6, 2 x 10^6, dan 2.5 x 10^6. Kemudian, kenaikan nilai rata-rata C_d tersebut masing-masing yaitu 1.120%, 1.301%, dan 1.396% pada bilangan *Reynolds* 1.6 x 10^6, 2 x 10^6, dan 2.5 x 10^6. Pada visualisasi kontur dapat terlihat bahwa *airfoil erosion* memiliki kontur tekanan yang bertambah pada bagian *upper chamber* dan berkurang pada bagian *lower chamber*. Hal tersebut juga terjadi seiring dengan meningkatnya bilangan *Reynolds*, sehingga dapat mengurangi gaya angkat *airfoil* NACA 0015. Kontur kecepatan aliran dan *streamline* juga menunjukkan aliran bersirkulasi yang lebih besar pada *airfoil* erosi yang dapat mempercepat *stall* 1° AoA pada *airfoil* erosion. Aliran bersirkulasi juga menjadi lebih besar seiring dengan meningkatnya bilangan *Reynolds* pada *airfoil*.

Kata kunci: CFD; erosi; NACA 0015; performa aerodinamika

Abstract

Airfoils that experience erosion with varying Reynolds numbers were studied using numerical methods to determine the effect on the performance of the NACA 0015 airfoil. A Computational Fluid Dynamics (CFD) approach has been used to this research. Reynolds Averaged Navier-Stokes (RANS) was used as the governing equation used in this research. The turbulence model used in this research was k-epsilon model. The Reynolds numbers used are 1.6 × 10^6, 2 × 10^6, and 2.5 × 10^6. This research proves that erosion can reduce the C_l value and increase the C_d value on the NACA 0015 airfoil. Increasing the Reynolds number can also reduce the average C_l value and increase the average C_d value. The decrease in the average value of C_l is 6.561%, 9.392%, and 9.803%, respectively, at Reynolds numbers 1.6 × 10^6, 2 × 10^6, and 2.5 × 10^6. Then, the average C_d value increase is 1.120%, 1.301%, and 1.396%, respectively, at Reynolds numbers 1.6 × 10^6, 2 × 10^6, and 2.5 × 10^6. The contour visualization shows that the airfoil erosion has a pressure contour that increases in the upper chamber and decreases in the lower chamber. This phenomenon also occurs as the Reynolds number increases so that it can reduce the lifting force of the NACA 0015 airfoil. The flow velocity and streamlined contours also show greater circulating flow on the erosion airfoil, which can accelerate the 1° AoA stall on the erosion airfoil. The circulating flow also becomes larger as the Reynolds number of the airfoil increases.

Keywords: *CFD; erosion; NACA 0015; aerodynamics performance*

1. Introduction

Energy is one of the most essential thing in human life. But, with the increasing energy demand, energy fulfillment has increased drastically, and fossil energy has become the most used energy these days [1]. Fossil fuel, commonly used in factories or commercials, can cause a damaged environment due to the pollutants the fossil fuel produces. As an alternative, green energy could be another good and environment-friendly alternative fuel. There are abundant choices among the applicants of green energy, for instance, wind turbines, photo voltaic, geothermal, etc [2]. The wind turbine

has an important component on its blades called airfoil. The blades of the wind turbine have an aerodynamic airfoil shape that could increase the lift coefficient on those blades, and it converts the kinetic energy in the wind into rotational mechanic energy on its blades [3]. But, in every day applied, the blades could be damaged due to the unwanted debris flying in the sky. For instance, bugs, sand particles, and birds that hit the blades can cause erosion on the surface. The erosion shape and dimension could vary and decrease the blade's performance [4].

Research on airfoils with various forms of damage to the airfoil surface has been widely carried out to determine the impact or effect of performance on the airfoil, like research conducted by Gharali et al. to determine the lift and drag coefficient under the impact of the erosion on the airfoil's leading edge with a Reynolds number of 1×10^6 and a reduced frequency (k) of 0.026. Variations in erosion thickness and length were investigated; the results showed that the most significant effect was shown for erosion thickness compared to erosion length. Variation of erosion with a thickness of 12% and a length of 14% has an average lift coefficient decrease of 17%, a thickness of 12% and a length of 4% has an average lift coefficient decrease of 20%, a thickness of 25% and a length of 14% has a decrease in lift coefficient an average of 34% [5]. Then, Wang et al. conducted CFD simulation research with varying pitting hole depths and Reynolds numbers. The results of this study show that the deeper the depth of the pitting hole causes a decrease in C_l/C_d, and the pitting hole has the greatest effect at an angle of attack of 8.1°, while it has a small effect when the angle of attack is smaller than 2.1°. when the pitting hole depth is below 0.5 mm, the aerodynamic performance of the S809 airfoil is more significantly affected by pitting erosion [6]. Another study was conducted by Sun et al. with semi-circular and cuboid erosion shapes on the leading edge of the airfoil with variations in depth of 0.3%c, 0.5%c, and 1%c. Erosion with a semi-circular shape and a depth of 0.3%c has the effect of decreasing C_l/C_d by 3.5% at AoA 8°, then decreases again at a depth of 0.5%c, and in the end, erosion with a depth of 1%c has a decrease in C_l/C_d of 26.3%. Cuboidal erosion significantly decreases C_l/C_d compared to semi-circular erosion at depths of 0.3%c and 0.5%c. However, at an erosion with depth of 1%c, the two forms of erosion tend to have insignificant differences in value [7].

The studies carried out above can provide information about the effect of erosion on airfoil performance with various erosion forms and types of airfoils. However, there are still many other things that can be investigated so that erosion's impact on airfoil performance can be understood more broadly. So, this research was carried out to determine further the impact of erosion by varying the Reynolds number. This way, changes in airfoil performance with erosion under the influence of changes in the Reynolds number can be further understood. This research will be carried out on the NACA 0015 model airfoil using a CFD approach and the k-epsilon model. The position of the airfoil angle of attack varies between 0° to 30° AoA. Different variations of the Reynolds number are also applied with Re values of 1.6×10^6, 2×10^6, and 2.5×10^6.

2. Material and Methodology

2.1. Erosion

Erosion is an event that generally occurs in wind turbine airfoils. Erosion can be caused by airborne debris and insects that hit the surface of the airfoil's leading edge. This impact causes weathering of the surface and creates a rough and perforated leading edge surface, which may lead to a decrease in the Airfoil's performance. On an eroded airfoil, the leading edge is the only area showing signs of erosion and will be the focus of modification in this numerical study [6]. In order to determine the differences in performance between baseline airfoil and eroded airfoil on the leading edge of the 0015 airfoil, an examination will be carried out during this research. The erosion model located on the leading edge of the airfoil has a thickness of 12%t (tA/t = 0.12) and a length of 14%c (hA/C = 0.14).

2.2. Governing Equations

A numerical method is applied to calculate the fluid flow around the airfoil profile based on solving the steady state equation, and it is called the RANS equation. These equations are written in equations (1) and (2). To define an equation of continuity for a fluid stream, Equation 1 will be used. Then equation (2) is used to write the momentum flow equation for fluid flow [8]. The direction of the fluid flow will be analysed with the assumption that it is only flowing on the X-axis.

$$\frac{\partial \rho}{\partial t} + \frac{\partial}{\partial x_i}(\rho u_i) = 0 \tag{1}$$

$$\frac{\partial}{\partial t}(\rho u_i) + \frac{\partial}{\partial x_i}(\rho u_i u_j) = -\frac{\partial p}{\partial x_i} + \frac{\partial}{\partial x_i}\left[\mu\left(\frac{\partial u_i}{\partial x_i} + \frac{\partial u_i}{\partial x_i} - \frac{2}{3}\delta_{ij}\frac{\partial u_i}{\partial x_i}\right)\right] + \frac{\partial}{\partial x_i}(-\rho x_i' u_i') \tag{2}$$

The standard k-epsilon equation for turbulence is used in this study. This equation was chosen because it can produce good values for turbulent flow with medium to high Reynolds number values. Equations (3) and (4) are used to write the turbulence equation used in this study. Equation (3) describes the transport equation for turbulence kinetic energy, and Equation 4 describes the specific dissipation rate equation [9].

$$\frac{\partial(\rho k)}{\partial t} + \frac{\partial(\rho k u_i)}{\partial x_i} = -\rho u_i' u_j' \frac{\partial u_j}{\partial x_i} - \rho\varepsilon + \frac{\partial}{\partial x_i}\left[\left(\mu + \frac{\mu_t}{\sigma_k}\right)\frac{\partial k}{\partial x_i}\right] + Gb \tag{3}$$

$$\frac{\partial(\rho\varepsilon)}{\partial t} + \frac{\partial(\rho\varepsilon u_i)}{\partial x_i} = C_{\varepsilon 1}\frac{\varepsilon}{k}\left(-\rho u_i' u_j' \frac{\partial u_j}{\partial x_i} + C_{\varepsilon 3} G_b\right) - C_{\varepsilon 2}\rho\frac{\varepsilon^2}{k} + \frac{\partial}{\partial x_i}\left[\left(\mu + \frac{\mu_t}{\sigma_\varepsilon}\right)\frac{\partial \varepsilon}{\partial x_i}\right] \tag{4}$$

2.3. Geometry

The geometry that will be used in this research is the NACA 0015 airfoil profile [10]. Then, two types of geometry will be used, NACA 0015 baseline and NACA 0015 erosion, which are given the erosion model on the leading edge posisition of the NACA 0015 airfoil. The geometry of the baseline airfoil and erosion airfoil are given in Figures 1 and 2. The baseline geometry is used to validate the data before Simulations are carried out on the modified geometry. The chord length (c) on the NACA 0015 baseline and NACA 0015 erosion airfoils is 1000 mm. The erosion model on the leading edge of the airfoil that will be simulated has a thickness tA of 0.04t and a length of 0.14c.

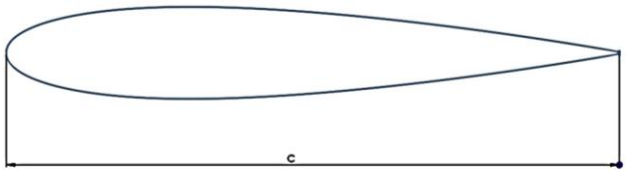

(a) NACA 0015 Baseline

(b) NACA 0015 Erosion

Figure 1. Airfoils of NACA 0015

2.4. Boundary Conditions

Boundary conditions are zones that become boundaries in a fluid system so that simulations can have exactly the same conditions as experiments in the real world. The domain of this study has two boundary conditions, with the center of the domain circle located at the trailing edge of the airfoil [11]. A velocity inlet with variations in speed of 23.3 m/s, 29.2 m/s, and 36.5 m/s is the first part of the domain. The Reynolds numbers that will be used in this research are 1.6×10^6, 2×10^6, and 2.5×10^6. The second part of the boundary condition is the outlet pressure with a value of 0 Pa. Then, the airfoil's boundary condition is considered as a wall with a non-slip condition. Figure 2 illustrates the detailed dimensions of the boundary conditions.

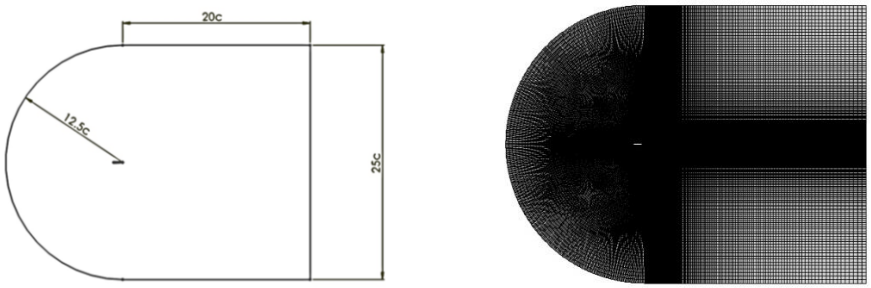

(a) Boundary condition (b) Boundary and mesh

Figure 2. Boundary condition and boundary mesh

2.5. Meshing

After drawing the geometry, the next step that will be taken is meshing or the discretization process of geometry into smaller parts for numerical calculations of an equation [12]. Elements in meshing consist of 2 types, namely quadrilateral elements and triangular elements. This research uses a structured mesh with quadrilateral elements because these elements offer a more accurate mesh option and have smaller errors. This mesh element also has smooth transitions between elements, so that type of mesh element can be used in this study. Meanwhile, meshes with triangle elements are suitable

for use in unstructured meshes, which have a more complex geometric structure because they have more flexible properties in forming complex geometries [13]. In this research, an independent mesh test to determine the most effective meshes for future simulations will be carried out.. The variations in the number of meshes that will be carried out by the mesh independence test are 1.6×10^6, 2×10^6, and 2.5×10^6.

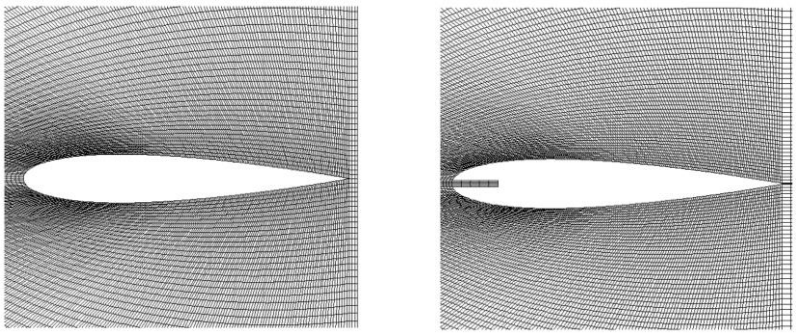

(a) NACA 0015 Baseline mesh (b) NACA 0015 Erosion mesh

Figure 3. Meshing of the airfoils

2.6. Aerodynamic of Airfoil

The aerodynamics of the airfoil are often discussed, with a view to discussing drag and lift force. The drag force can be considered as an aerodynamic force that is aligned in the same direction as a fluid flow vector. In addition, it may be considered to be a lift force if the force vector is in the same direction as that of the fluid flow [14]. Drag and lift force are generally expressed as a measure without dimension, referred to as the drag and lift coefficient [15]. The formulas for both can be seen in Equations (5) and (6).

$$C_d = \frac{2d}{\rho u^2 c} \tag{5}$$

$$C_l = \frac{2l}{\rho u^2 c} \tag{6}$$

3. Results and Discussion

The mesh independence test in this research was checked to ensure convergence and the number of errors. There is a method called Richardson Extrapolation, which was generalized by Roache [16]. In the mesh independence test that was carried out in this study, x component velocity values were taken into account at coordinates of x=0.5 and y=0.15. The mesh independence test will be performed in an order of 1.8, which corresponds to a ratio of variation 2 for the meshes. A safety factor of 1.25 will be used to test the mesh independently. For fine mesh and coarse mesh, the grid convergence index has been calculated as 1.100% and 2.4948% respectively. In order to conclude that the mesh variations are in the convergence index with the respective mesh errors of 0.8632%, 1.9568%, and 4.4359%, the final result of the mesh independence test is close to 1. Based on Figure 4, the fine mesh has values that are close to the parameters, so the mesh is used for further simulations.

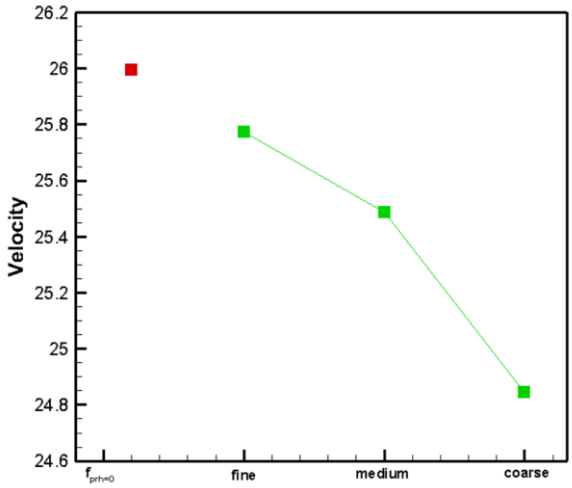

Figure 4. Mesh independence test result

Validation in this research is done to ensure the simulation model has values close to the experimental results. Validation was carried out by comparing C_l and C_d NACA 0015 baseline data with data from experimental studies conducted by Kekina and Suvanjumrat [17]. Validation was compared at a Reynolds number of 1×10^6. Figure 5a shows the comparison C_l results of CFD data and experimental data. In general, the trend pattern of all C_l curve data shows similarities. At an AoA of less than 10°, data between experiments and CFD show errors that tend to be smaller, whereas after AoA is more than 10°, there are errors that tend to be larger. This is caused by turbulence phenomena that are difficult to predict in the AoA. The graph of changes in C_d can be seen in Figure 5b. The experimental and CFD curves show similar data trends in changes in C_d towards AoA. The difference in C_d values between the baseline and experimental airfoils was not too significant when AoA <7°, but there was a significant difference after the AoA angle.

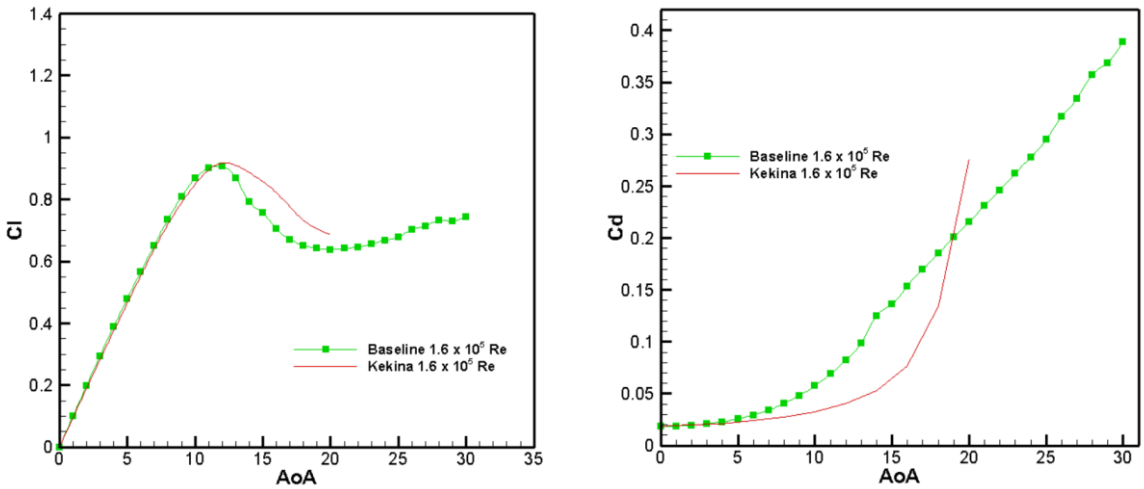

(a) C_l validation (b) C_d validation

Figure 5. Airfoil validation

The simulation results are shown in Figure 7 by comparing C_l values between the baseline and eroded airfoil, which is compared with variations in Reynolds coefficients, to show how it has worked out. The effect of varying the Reynolds number on airfoil erosion shows values that are not significantly different when AoA<10° and AoA>21°. The C_l value also does not significantly differ in each AoA on the baseline airfoil. Variations in the Reynolds number also show a tendency to increase in the C_l value as the Reynolds number increases in the airfoil. This can happen because the higher the Reynolds number, the greater the wind flow speed, providing an even greater lifting force. The average decrease in C_l value between baseline airfoil and eroded airfoil at Reynolds numbers 1.6 × 10⁶, 2 × 10⁶, and 2.5 × 10⁶ is 6.561%, 9.392%, and 9.803%, respectively It can be concluded that between the baseline airfoil and the eroded airfoil, the Reynolds number is higher which implies a greater decrease in average C_l values.. The eroded airfoil stalls 1° faster compared to the baseline airfoil. The eroded airfoil stalls at AoA 11°, while the baseline airfoil stalls at AoA 12°. After the airfoil stalls, the C_l value tends to decrease further because the fluid flow circulates on the larger airfoil and can reduce the C_l value on the airfoil.

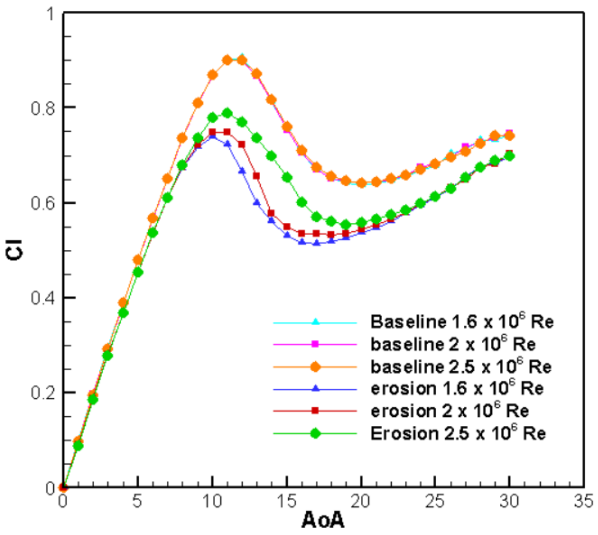

Figure 6. C_l of the airfoils

The results of the simulation are shown in Figure 8 in the form of C_d values for variations in AoA and Reynolds number. The effect of erosion on the airfoil has been tested and proven to increase the C_d value on the NACA 0015 erosion airfoil. The graph shows that the increase in C_d values has the same trend between eroded airfoil and baseline airfoil, with the C_d value slightly increasing in eroded airfoil. The increase in the average C_d value between baseline airfoil and eroded airfoil is 1.120%, 1.301%, and 1.396% at Reynolds numbers 1.6 × 10⁶, 2 × 10⁶, and 2.5 × 10⁶. For each Reynolds number, the average increase in C_d value between the baseline airfoil and the eroded airfoil is not significantly different. The erosion effect can increase flow separation, thereby increasing the C_d value on the airfoil. The flow separation in the upper chamber airfoil after the stall can also increase the C_d value, which is higher than before the stall.

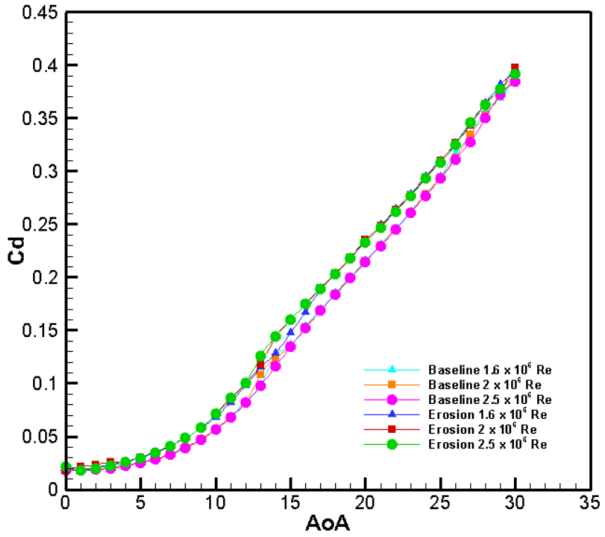

Figure 7. C_d of the airfoils

Figure 9 provides a visual representation of fluid flow and velocity distribution around both the baseline NACA 0015 and the NACA 0015 erosion airfoil, while also showing the variations in the Reynolds number. Visualization is carried out at AoA 15º by depicting speed and streamline contours. This visualization can make it easier for observers to see the phenomena around the airfoil. As seen in the image, eroded airfoil significantly influences flow circulation compared to the baseline airfoil. The flow separation point in eroded airfoil tends to be earlier than the baseline airfoil. The upper chamber of the erosion airfoil has a larger circulation compared to its baseline, and there is an additional flow from the trailing edge. The circulating flow, which tends to be greater, can have a stalling effect on eroded airfoil, which occurs faster than the baseline airfoil. Variations in the Reynolds number also affect the circulation behavior of the airfoil. The higher the Reynolds number, the earlier the flow separation point and the greater the flow circulation.

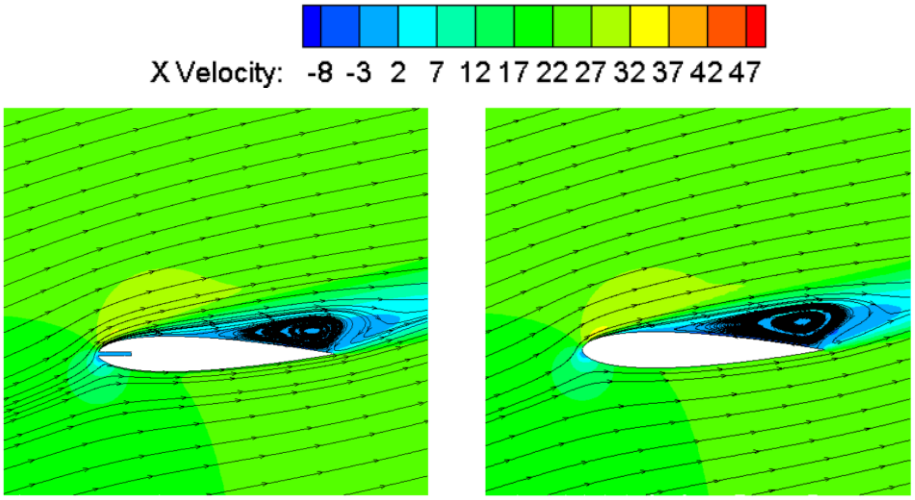

(a) Erosion AoA 15° Re 1.6 x 10^6 (b) Baseline AoA 15° Re 1.6 x 10^6

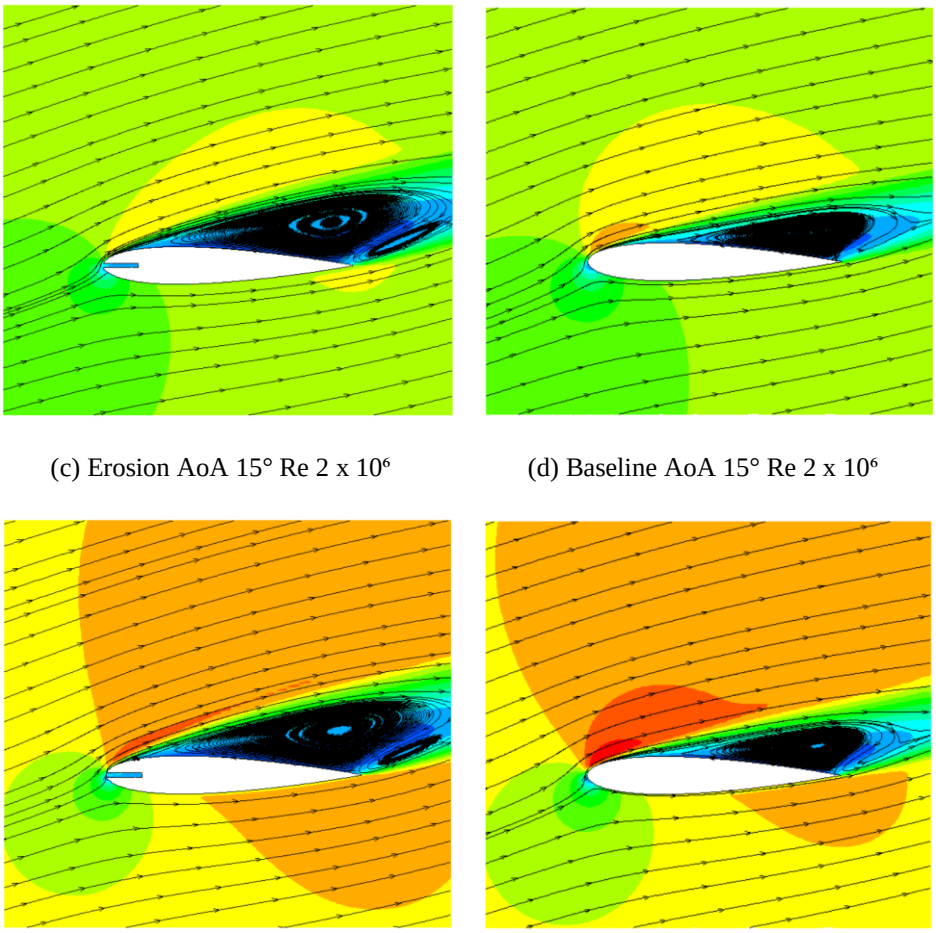

(c) Erosion AoA 15° Re 2 x 10^6 (d) Baseline AoA 15° Re 2 x 10^6

(e) Erosion AoA 15° Re 2.5 x 10^6 (f) Baseline AoA 15° Re 2.5 x 10^6

Figure 8. Velocity contour and streamlines

Figure 10 shows a visual representation of the pressure contours surrounding both the baseline NACA 0015 airfoil and the NACA 0015 erosion airfoil, showing variations in the Reynolds number. The contour visualization occurs when the airfoil has an AoA of 15°. This image shows that the pressure contour on the airfoil is greater in the lower chamber than in the upper chamber, so the pressure difference can exert a lift force on the airfoil. The effect of erosion is proven to reduce pressure in the lower chamber and increase pressure in the upper chamber airfoil. This phenomenon can be seen in changes in the pressure distribution in the airfoil section. Thus, this can cause the lifting force on the eroded airfoil to decrease. The pressure contour of the airfoil is also affected by variations in Reynolds numbers. The Reynolds numbers increase the pressure in the low chamber airfoil and decrease the pressure in the high chamber airfoil. So it can increase the lift force on the airfoil.

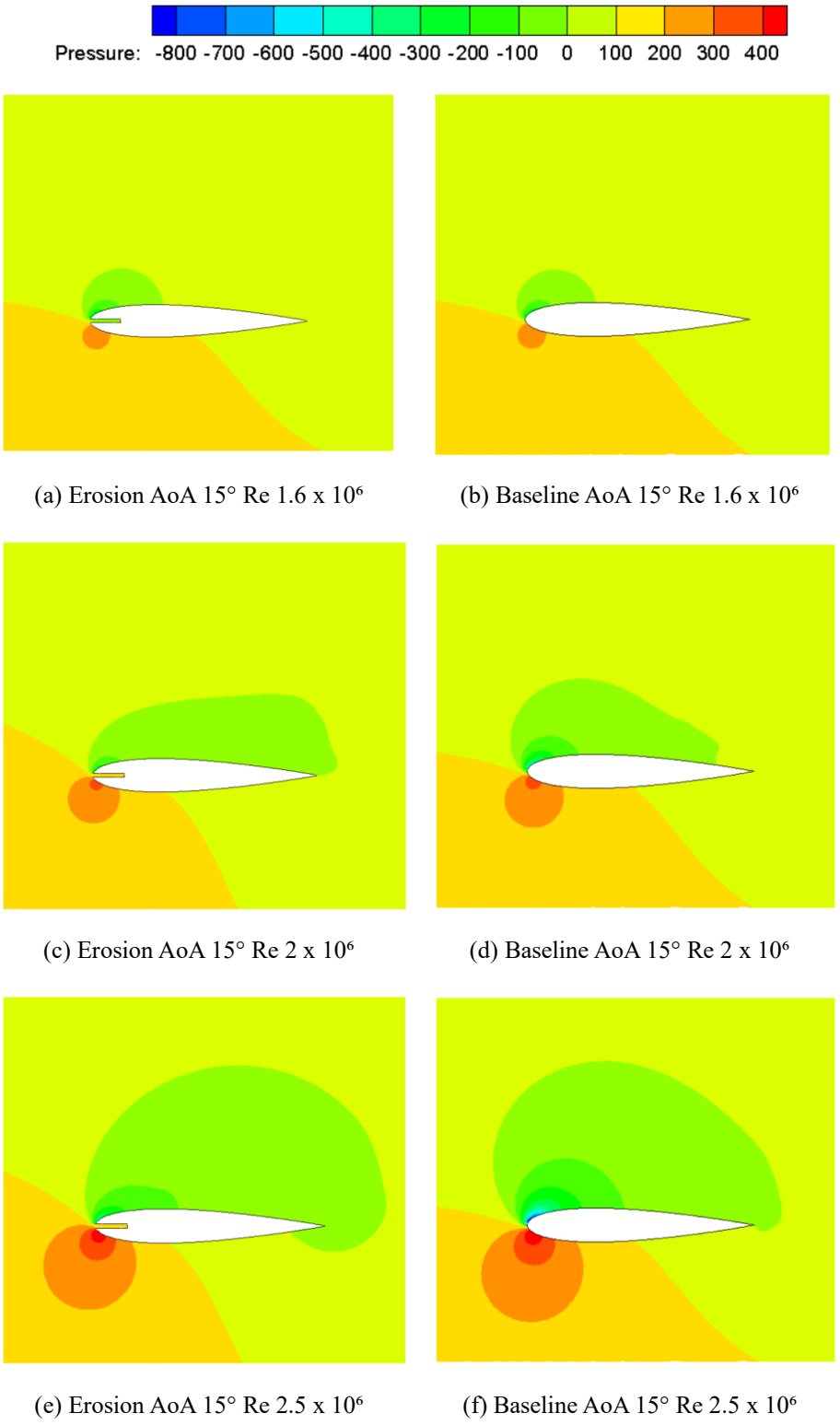

(a) Erosion AoA 15° Re 1.6 x 10^6 (b) Baseline AoA 15° Re 1.6 x 10^6

(c) Erosion AoA 15° Re 2 x 10^6 (d) Baseline AoA 15° Re 2 x 10^6

(e) Erosion AoA 15° Re 2.5 x 10^6 (f) Baseline AoA 15° Re 2.5 x 10^6

Figure 9. Pressure contour

4. Conclusion

Erosion on the NACA 0015 airfoil has been proven to change the C_l and C_d values compared to airfoils that do not experience erosion. Airfoils that experience erosion are proven to cause a decrease in C_l values and can increase C_d values compared to airfoils that do not experience erosion. Variations in the value of the Reynolds number also influence the performance of the airfoil. Variations in the Reynolds number show that the greater the value of the Reynolds number, the greater the decrease in the average C_l value. These values are 6.561%, 9.392%, and 9.803%, respectively, at Reynolds numbers of 1.6×10^6, 2×10^6, and 2.5×10^6. Then, variations in the Reynolds number have a less significant effect on changes in the C_d value, with an average value increase of 1.120%, 1.301%, and 1.396% at Reynolds numbers 1.6×10^6, 2×10^6, and 2.5×10^6. This can be seen in the visualization of the airfoil's pressure, velocity, and streamline contours. Eroded airfoils tend to have greater circulation flow than baseline airfoils. The eroded airfoil pressure contour also increases in the upper chamber and decreases in the lower chamber. Changes in performance caused by variations in the Reynolds number can also be caused by circulating flow, which tends to be greater as the Reynolds number increases. The higher Reynolds number may also lead to increased pressure in the upper chamber and reduced pressure at the lower chamber, limiting airfoil lift force. Then, the stall phenomenon in eroded airfoil occurs at 1° AoA faster than airfoils that do not experience erosion. This can be caused by flow separation occurring more quickly in eroded airfoil compared to the baseline airfoil.

References

[1] Omer, A.M. Green Energies and The Environment. Renewable and Sustainable Energy Reviews. 2008 September; 12(7): p. 1789–821.

[2] Loutun, M.J.T., Didane, D.H., Batcha, M.F.M., Abdullah, K., Ali, M.F.M., Mohammed, A.N., et al. 2D CFD Simulation Study on The Performance of Various NACA Airfoils. CFD Letters. 2021 Apr 1; 13(4): p. 38–50.

[3] Wagner, H-J. Introduction to Wind Energy Systems. In Proceedings of the 4th Course of the Joint EPS-SIF International School on Energy. EDP Sciences; 2018.

[4] Li, D., Zhao, Z., Li, Y., Wang, Q., Li, R., Li, Y. Effects of The Particle Stokes Number on Wind Turbine Airfoil Erosion. Applied Mathematics and Mechanics (English Edition). 2018 May 1; 39(5): p. 639–52.

[5] Gharali, K., and Johnson, D.A. Numerical Modeling of An S809 Airfoil Under Dynamic Stall, Erosion and High Reduced Frequencies. Applied Energy. 2012;93: p. 45–52.

[6] Wang, Y., Hu, R., Zheng, X. Aerodynamic Analysis of an Airfoil With Leading Edge Pitting Erosion. Journal of Solar Energy Engineering, Transactions of the ASME. 2017 Dec 1;139(6).

[7] Sun, J., Zhang, S., Cao, P., Qi, L. Influence of Blade Maximum Thickness on Airfoil Performance With Varied Leading Edge Erosion Rate. Front Energy Res. 2023 Jan 4; 10.

[8] Aftab, S. M. A., Ahmad. K. A. CFD Study on NACA 4415 Airfoil Implementing Spherical and Sinusoidal Tubercle Leading Edge. PLoS One. 2017 Aug 1;12(8).

[9] Darbandi, M., Setayeshgar, A., Vakili, S., Schneider, G. E. Modification of Standard k-Epsilon Turbulence Model for Multi-Element Airfoil Application Using Optimization Technique. 2006.

[10] Abd Aziz, P.D., R Mohamad, A.K., Hamidon, F., Mohamad, N., Salleh, N., Mohd Yunus, N. A Simulation Study on Airfoils Using VAWT Design for Low Wind Speed Application. In Proceeding of 2014 4th International Conference on Engineering Technology and Technopreneuship (ICE2T). IEEE. 2015 January 12.

[11] Julian, J., Iskandar, W., and Wahyuni, F. Computational Fluid Dynamics Analysis Based on The Fluid Flow Separation Point on The Upper Side of The NACA 0015 Airfoil with The Coefficient of Friction. Jurnal Media Mesin. 2022; 23(2).

[12] Sack, J.R., and Urrutia, J. Handbook of Computational Geometry. Elsevier; 2000.

[13] Chen, X., Liu, J., Yan, J., Wang, Z., Gong, C. An Improved Structured Mesh Generation Method Based on Physics-informed Neural Networks. 2022 Oct 17; Available from: http://arxiv.org/abs/2210.09546

[14] Julian, J., Iskandar, W., and Wahyuni, F. Aerodynamics Improvement of NACA 0015 by Using Co-Flow Jet. International Journal of Marine Engineering Innovation and Research. December 2022; 7(4): p. 284-291.

[15] Julian, J., Iskandar, W., and Wahyuni, F. Effect of Single Slat and Double Slat on Aerodynamic Performance of NACA 4415. International Journal of Marine Engineering Innovation and Research. June 2022; 7(2): p. 93-100.

[16] Boache PJ. Perspective: A Method for Uniform Reporting of Grid Refinement Studies [Internet]. 1994. Available from: http://fluidsengineering.asmedigitalcollection.asme.org/

[17] Kekina, P., Suvanjumrat, C. A Comparative Study on Turbulence Models for Simulation of Flow Past NACA 0015 Airfoil Using OpenFOAM. In Proceeding of 2016 the 3rd International Conference on Mechatronics and Mechanical Engineering (ICMME 2016).